H+j Production at the LHC

Roberto Bonciani

Dipartimento di Fisica, Sapienza - Università di Roma

INFN - Sezione di Roma

In Collaboration with: V. Del Duca, M. Becchetti, H. Frellesvig, M. Hidding, V. Hirschi, F. Moriello, G. Salvatori, A. Schweitzer, G. Somogyi, and F. Tramontano

QCD meets EW, CERN 5-9 February 2024

Plan of the talk

- General Introduction
- Theoretical Predictions in the literature
- Some details about the calculation of H+j

Higgs Production at the LHC

- Higgs boson detected for the first time in 2012 by ATLAS and CMS collaborations at CERN. Since that date effort of the community for the study of the properties of this particle Standard Model like?

- Higgs boson produced at LHC in many production channels:

gluon gluon fusion (ggF)
vector boson fusion (VBF),
associated production with a vector boson
associated production with a t-tbar pair

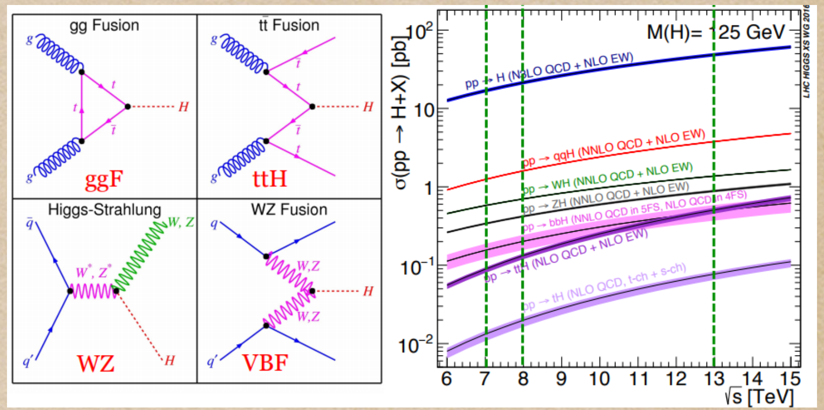

- Although gluon-fusion is a loop-induced process, because the Higgs does not couple directly to gluons, the CS in this channel is one order of magnitude bigger than VBF

- Since gluon-fusion proceeds via a loop of heavy quarks, it is sensible to possible new heavy states running into the loops: → portal to NP effects

In the following, focus on ggF

Higgs Production at the LHC

- LO prediction end of the '70

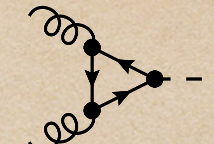

H. M. Georgi, S. L. Glashow, M. E. Machacek, D. V. Nanopoulos, Phys. Rev. Lett. 40 (1978) 642

- NLO QCD corrections in the '90: increase of the CS by 50-70%; scale dependence 30%

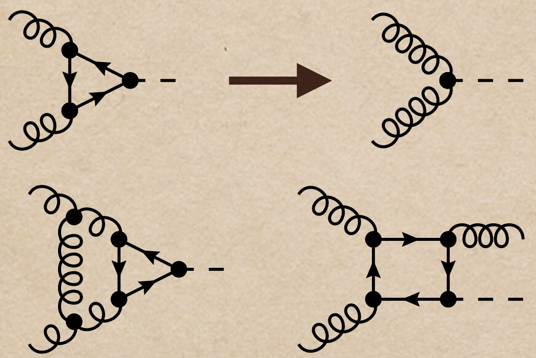

S. Dawson, Nucl. Phys. B 359 (1991) 283
A. Djouadi, M. Spira, P. M. Zerwas, Phys. Lett B 264 (1991) 440

D. Graudenz, M. Spira, P. M. Zerwas, Phys. Rev. Lett. 70 (1993) 1372
M. Spira, A. Djouadi, D. Graudenz, P. M. Zerwas, Nucl. Phys. B 453 (1995) 17

- NNLO QCD corrections in 2002: further increase of the CS by 15% w.r.t. NLO; reduction of the scales dependence to 15-20%

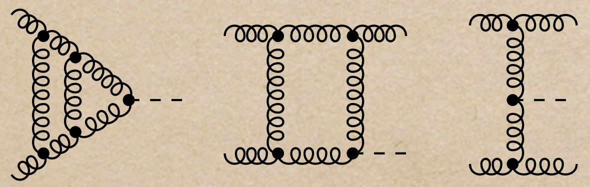

R. V. Harlander, W. B. Kilgore, Phys. Rev. Lett. 88 (2002) 201801
C. Anastasiou, K. Melnikov, Nucl. Phys. B 646 (2002) 220
V. Ravindran, J. Smith, W. L. Van Neerven, Nucl. Phys. B 665 (2003) 325

- The dynamics of Higgs production is governed by the soft region, where the partonic c.m. energy is near mH (validity of infinite top mass limit). Important Soft-gluon resummation: 6% increase of the CS; residual theoretical uncertainty 10%

S.Catani, D. De Florian, M. Grazzini, P. Nason, JHEP 0307 (2003)028

Higgs Production at the LHC

- The state-of-the-art, up to some years ago, was represented by the total ggF CS known at the NNNLO in QCD! Nice convergence of the pt series: moderate increase of the central value but sizeable reduction in the scale dependence w.r.t. NNLO. At 13 TeV and Higgs mass of 125 GeV

$$\sigma = 48.58\ \text{pb}^{+2.22\ \text{pb}\ (4.56\%)}_{-3.27\ \text{pb}\ (-6.72\%)} \pm 1.56\ \text{pb}(3.2\%)$$

← It includes mass effects and EW

C. Anastasiou, C. Duhr, F. Dulat, F. Herzog, B. Mistlberger, Phys. Rev. Lett. 114 (2015) 212001
C. Anastasiou, C. Duhr, F. Dulat, E. Furlan, T. Gehrmann, F. Herzog, A. Lazopoulos, B. Mistlberger, JHEP 1615 (2016) 058
B. Mistlberger, JHEP 05 (2018) 028

- The calculation was done in the $m_t \to \infty$ limit

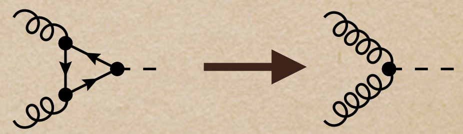

- Inclusive calculation (integration over the whole phase space) with reverse unitarity

C. Anastasiou, K. Melnikov, Nucl. Phys. B646 (2002) 220

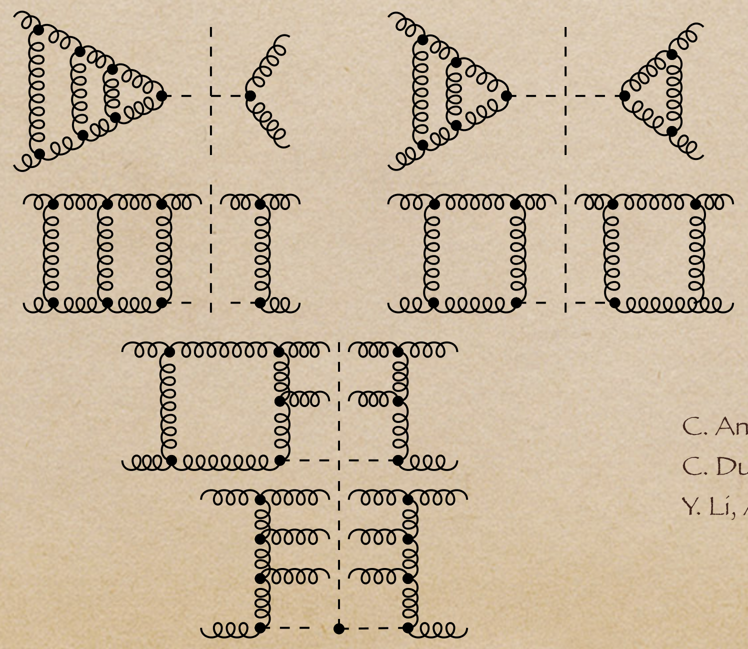

P. A. Baikov, K. G. Chetyrkin, A. V. Smirnov, V. A. Smirnov, M. Steinhauser, PRL 102 (2009)
T. Gehrmann, E. W. N. Glover, T. Huber, N. Ikizlerli, C. Studerus, JHEP 06 (2010) 094

C. Duhr, T. Gehrmann, M. Jaquier, JHEP 02 (2015) 077
F. Dulat, B. Mistlberger, arXiv 1411.3586
W. B. Kilgore, PRD89 (2014) 073008

C. Anastasiou, C. Duhr, F. Dulat, B. Mistlberger, JHEP 07 (2013)
C. Duhr, T. Gehrmann, Phys. Lett. B 727 (2013)
Y. Li, A. Von Manteuffel, R. Schabinger, H. X. Zhu, PRD91 (2015) 032008

It turns out that this is an interesting obs by itself, H+j

Higgs Production at the LHC

- The NNNLO is an inclusive calculation (integration over the whole phase space). It is important to be able to give predictions that implement the experimental cuts, and more differential obs

- Expansion near threshold: Rapidity distribution

F. Dulat, B. Mistlberger, A. Pelloni, JHEP 1801 (2018) 145; Phys.Rev.D 99 (2019) 3, 034004

- Extension at NNNLO of Qt subtraction: fiducial CS and rapidity distribution

L. Cieri, X. Chen, T. Gehrmann, E. W. N. Glover, A. Huss, JHEP 02 (2019) 096

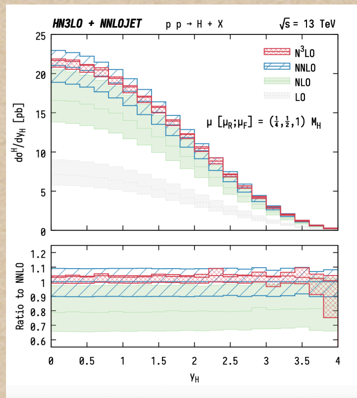

- Differential CS NNNLO + resummation up to NNNLL (Qt and "Projection to Born")

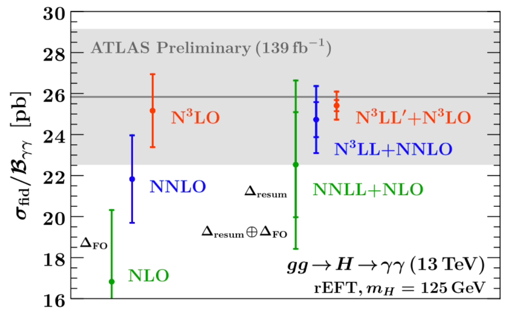

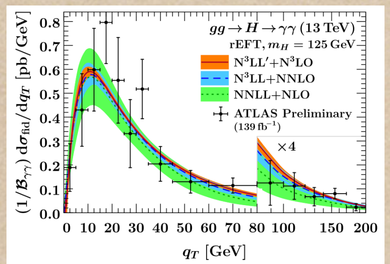

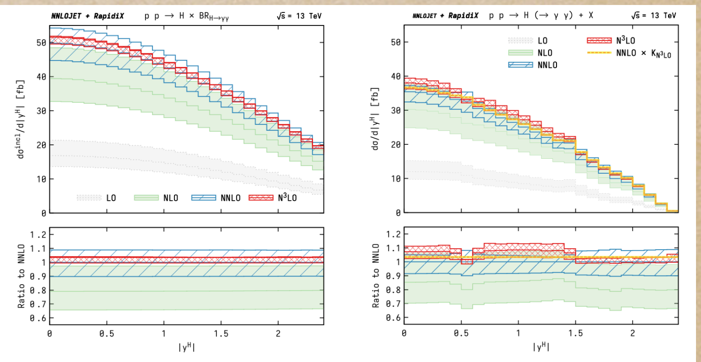

G. Billis, B. Dehnadi, M. A. Ebert, J. K. L. Michel, F. J. Tackmann, PRL 127 (2021) 072001
X. Chen, T. Gehrmann, E. W. N. Glover, A. Huss, B. Mistlberger, A. Pelloni, PRL 127 (2021) 072002

Higgs Production at the LHC

- Due to the extreme accuracy of the NNNLO prediction, it was/is important to look at possible "effects" at the percent level!
- This "best prediction" is based on: up to NNNLO QCD (rescaled by exact LO) + EW corrections at LO in the e.m. coupling + approx mass contributions. Important remaining effects are:
    - Mass effects: higher-order exact QCD corrections, with top and bottom contributions These effects were estimated to be of the order of 1%
    - QCD-EW in ggF: the LO EW contributions turned out to be sizeable (2% of CS); to the NLO is assigned an error of 1%
    - QCD-EW corrections in other channels (qg and qqbar): these contributions that can in principle be of the same order of magnitude (or slightly smaller) of the previous one
    - Errors due to "incorrect use of the PDFs": mismatch in perturbative order of the evolution.

Higgs Production at the LHC

- The complete NNLO in QCD with finite heavy-quark masses was completed recently

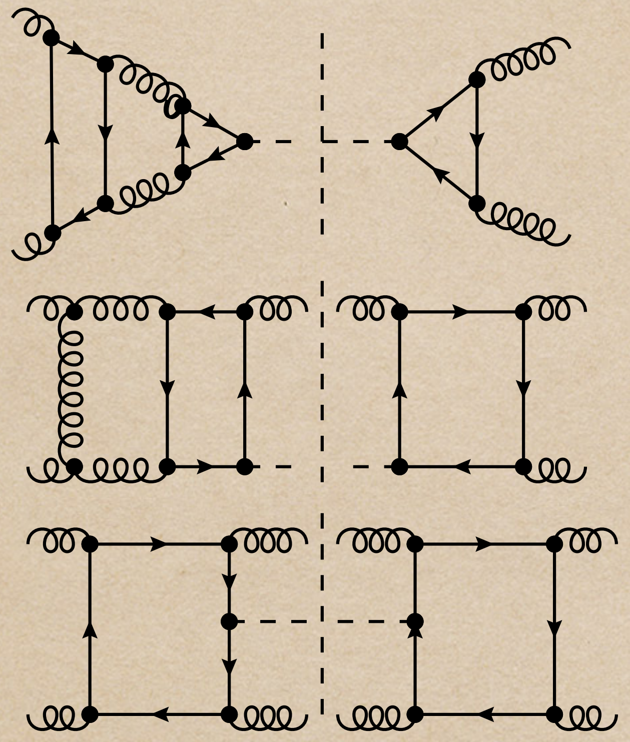

M. Niggetiedt, M. Czakon, JHEP 05 (2020) 149
M. Czakon, R. V. Harlander, J. Klappert, M. Niggetiedt, PRL 127 (2021) 162002
M. Niggetiedt, J. Usovitch, 2312.05297
M. Czakon, F. Eschment, M. Niggetiedt, R. Poncelet, T. Schellenberger, 2312.09896

S. P. Jones, M. Kerner, G. Luisoni, Phys. Rev. Lett. 120 (2018) 162001
R.B., V. Del Duca, H. Frellesvig, M. Hidding, V. Hirschi, F. Moriello, G. Salvatori, G. Somogyi, F. Tramontano, Phys.Lett.B 843 (2023) 137995

V. Del Duca, W. Kilgore, C. Oleari, C. Schmidt, D. Zeppenfeld, PRL 87 (2001) 122001
Nucl. Phys. B616 (2001) 367

Calc Analytically complex: elliptic integrals
Can be done in power expansion ….

- The IR subtraction was calculated with "Residue subtraction", it can be calculated with Qt …

RESULTS :

Higgs Production at the LHC

- The total effect of TOP corrections is -0.32% at 13 TeV (w.r.t. HEFT that takes into account already LO mt)
- gg-channel ok, but qg and qq are not described well by HEFT

TABLE I. Effects of a finite top-quark mass on the total hadronic Higgs-boson production cross section for the LHC at 13 TeV and 8 TeV, separately for the partonic channels and including Monte Carlo integration error estimates. Results obtained with the PDF set `NNPDF31_nnlo_as_0118` [1], renormalization and factorization scales $\mu_R = \mu_F = M_H/2$, Higgs-boson mass $M_H = 125$ GeV, and top-quark mass $M_t = \sqrt{23/12} \times M_H \approx 173.055$ GeV. The NNLO cross section within HEFT ($\sigma^{\rm NNLO}_{\rm HEFT}$) has been obtained with `SusHi` [2,3] and is split into contributions from the individual orders in α_s.

	$\sigma^{\rm NNLO}_{\rm HEFT}$ [pb]	$(\sigma^{\rm NNLO}_{\rm exact} - \sigma^{\rm NNLO}_{\rm HEFT})$ [pb]		
Channel	$\mathcal{O}(\alpha_s^2) + \mathcal{O}(\alpha_s^3) + \mathcal{O}(\alpha_s^4)$	$\mathcal{O}(\alpha_s^3)$	$\mathcal{O}(\alpha_s^4)$	$(\sigma^{\rm NNLO}_{\rm exact}/\sigma^{\rm NNLO}_{\rm HEFT} - 1)$ [%]
		$\sqrt{s} = 8$ TeV		
gg	$7.39 + 8.58 + 3.88$	$+0.0353$	$+0.0879 \pm 0.0005$	$+0.62$
qg	$0.55 + 0.26$	-0.1397	-0.0153 ± 0.0002	-19
qq	$0.01 + 0.04$	$+0.0171$	-0.0191 ± 0.0002	-4
Total	$7.39 + 9.14 + 4.18$	-0.0873	$+0.0535 \pm 0.0006$	-0.16
		$\sqrt{s} = 13$ TeV		
gg	$16.30 + 19.64 + 8.76$	$+0.0345$	$+0.2431 \pm 0.0020$	$+0.62$
qg	$1.49 + 0.84$	-0.3696	-0.0408 ± 0.0005	-18
qq	$0.02 + 0.10$	$+0.0322$	-0.0501 ± 0.0006	-15
Total	$16.30 + 21.15 + 9.70$	-0.3029	$+0.1522 \pm 0.0021$	-0.32

M. Czakon, R. V. Harlander, J. Klappert, M. Niggetiedt, PRL 127 (2021) 162002

- The total effect of T-B interference at 13 TeV is to reduce the CS by 2pb (which means -4.2%)
- This reduction is bigger than the effect of the sole top

TABLE I. Effects of interference of bottom- and top-quark amplitudes on Higgs production in the gluon-fusion channel at LHC @ 8 TeV and 13 TeV. The results are obtained with the `NNPDF31_nnlo_as_0118` [43] PDF set with a Higgs mass of $m_H = 125$ GeV and quark masses of $m_t = \sqrt{23/12}\, m_H \approx 173.055$ GeV and $m_b = \sqrt{1/684}\, m_H \approx 4.779$ GeV. The calculation was performed at a central scale of $\mu_F = \mu_R = m_H/2$. The scale uncertainties were determined with seven-point variation. The same scale setting was used in the numerator and denominator in the ratio presented in the last column. The HEFT values have been obtained with `SusHi` [44, 45].

Order	$\sigma_{\rm HEFT}$ [pb]	$(\sigma_t - \sigma_{\rm HEFT})$ [pb]	$\sigma_{t\text{-}b\text{-interference}}$ [pb]	$\sigma_{t\text{-}b\text{-interference}}/\sigma_{\rm HEFT}$ [%]
		$\sqrt{s} = 8$ TeV		
$\mathcal{O}(\alpha_s^2)$	$+7.39$	–	-0.895	
LO	$7.39^{+1.98}_{-1.40}$	–	$-0.895^{+0.17}_{-0.24}$	-12
$\mathcal{O}(\alpha_s^3)$	$+9.14$	-0.0873	$-0.269(2)$	
NLO	$16.53^{+3.63}_{-2.73}$	$-0.0873^{+0.030}_{-0.052}$	$-1.16^{+0.10}_{-0.08}$	$-7.0^{+1.0}_{-0.8}$
$\mathcal{O}(\alpha_s^4)$	$+4.19$	$+0.0523(2)$	$+0.167(3)$	
NNLO	$20.72^{+1.84}_{-2.06}$	$-0.350(2)^{+0.048}_{-0.013}$	$-0.998(4)^{+0.12}_{-0.05}$	$-4.8^{+0.9}_{-0.8}$
		$\sqrt{s} = 13$ TeV		
$\mathcal{O}(\alpha_s^2)$	$+16.30$	–	-1.975	
LO	$16.30^{+4.36}_{-3.10}$	–	$-1.98^{+0.37}_{-0.53}$	-12
$\mathcal{O}(\alpha_s^3)$	$+21.14$	$-0.3029(2)$	$-0.447(4)$	
NLO	$37.44^{+8.42}_{-6.29}$	$-0.3029(2)^{+0.10}_{-0.17}$	$-2.42^{+0.19}_{-0.12}$	$-6.5^{+0.9}_{-0.8}$
$\mathcal{O}(\alpha_s^4)$	$+9.72$	$+0.147(1)$	$+0.434(8)$	
NNLO	$47.16^{+4.21}_{-4.77}$	$-0.158(1)^{+0.13}_{-0.03}$	$-1.99(1)^{+0.30}_{-0.15}$	$-4.2^{+0.9}_{-0.8}$

M. Czakon, F. Eschment, M. Niggetiedt, R. Poncelet, T. Schellenberger, 2312.09896

Higgs Production at the LHC

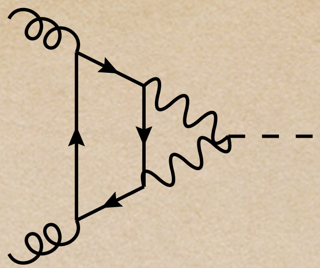

- LO prediction enhances the total CS by almost 2%:
  the light-fermion component gives 98% of the correction

U. Aglietti, R.B., G. Degrassi, A. Vicini, Phys. Lett. B 595 (2004) 432
G. Degrassi, F. Maltoni, Phys. Lett. B 600 (2004) 255
S. Actis, G. Passarino, C. Sturm, S. Uccirati, Phys. Lett. B 670 (2008) 12

- NLO QCD-EW: due to the behaviour of the LO, the focus is on light-quark contribution

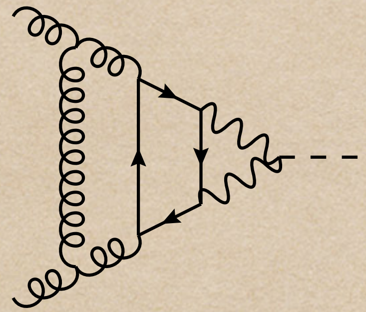

M. Bonetti, K. Melnikov, L. Tancredi, Nucl. Phys. B 916 (2017) 709;
Phys. Rev. D 97 (2018) 056017

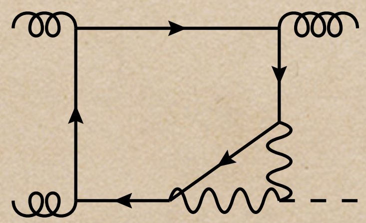

M. Bonetti, E. Panzer, V. A. Smirnov, L. Tancredi, JHEP 11 (2020) 045
M. Becchetti, R.B., V. Del Duca, V. Hirschi, F. Moriello, A. Schweitzer,
Phys. Rev. D 103 (2021) 054037
M. Becchetti, F. Moriello, A. Schweitzer, JHEP 04 (2022) 139

$$\sigma_{gg\to H+X}^{(\alpha_S^2\alpha^2)} = 0.68739^{+23.4\%+2.0\%}_{-17.3\%-2.0\%}\, pb$$

$$\sigma_{gg\to H+X}^{(\alpha_S^2\alpha^2+\alpha_S^3\alpha^2)} = 1.467(2)^{+18.7\%+2.0\%}_{-14.6\%-2.0\%}\, pb$$

4.8% of the gg @ NLO HEFT

QCD meets EW, CERN 5-9 February 2024

H+jet

- Phenomenological importance
  - recoiling against the Higgs system, the jet can reveal a possible substructure of the Higgs boson, therefore distributions are instrumental for the search of NP effect
  - exclusive observables enable to decouple different anomalous couplings of the Higgs to known particles of the SM (Yukawa and effective coupling to gluons), where inclusive quantities are sensible to their sum.

Harlander, Neumann '13
Azatov et al. '15, Grojean et al. '14

- Computational importance
  - H+j is a NLO QCD computation, i.e. the number of Feynman diagrams is quite reduced (~100 ??); however their computation is quite complicated due to the presence of 4 scales (s, t, m_t and p_H)
  - interesting playground for computational techniques, study of the functional structure of Feynman diagrams etc ...

H+jet

- The pt distribution is known at LO in the full theory and at higher orders in the heavy-top limit

R. K. Ellis,I. Hinchliffe, M. Soldate, J. J. Van der Baj, Nucl. Phys. B 297 (1988) 221
U. Baur, E. W. N. Glover, Nucl. Phys. B 339 (1990) 38

- In HEFT (infinite top mass) the NNLO QCD corrections are known

R. Boughezal, F. Caola, K. Melnikov, F. Petriello, M. Schulze, JHEP06 (2013) 072
Phys. Rev. Lett. 115 (2015) 082003
X. Chen, T. Gehrmann, E. W. N. Glover, M. Jaquier, Phys. Lett. B 740 (2015) 147
R. Boughezal, C. Focke, W. Giele, X. Liu, F. Petriello, Phys. Lett. B748 (2015) 5

- Power in $1/m_t^2$ corrections at NLO in QCD were also calculated

R. Harlander,T. Neumann, K. J. Ozeren, M. Wiesemann, JHEP 08 (2012) 139
T. Neumann, M. Wiesemann, JHEP 11 (2014) 150

- Small bottom mass interference effects and asymptotic $p_{t,H} \geq 400\ \mathrm{GeV}$ were also calculated

K. Melnikov, L. Tancredi, C. Wever, JHEP 11 (2016) 104; Phys. Rev. D95 (2017) 054012
R. Mueller, D. G. Ozturk, JHEP 08 (2016) 055
J. M. Lindert, K. Melnikov, L. Tancredi, C. Wever, Phys. Rev. Lett. 118 (2017) 252002
K. Kudashkin, K. Melnikov, C. Wever, JHEP 02 (2018) 135
J. M. Lindert, K. Kudashkin, K. Melnikov, C. Wever, Phys. Lett. B782 (2018) 210

H+jet

- H+j was computed at NLO in QCD with the full TOP mass dependence

S. P. Jones, M. Kerner, G. Luisoni, Phys. Rev. Lett. 120 (2018) 162001
X.Chen, A.Huss, S.P.Jones, M.Kerner, J.N.Lang, J.M.Lindert, H.Zhang, JHEP 03 (2022) 096

  - Everything except virtual corrections are calculated analytically
  - VIRTUAL: reduction to the Master Integrals, the MIs basis is chosen to be composed by quasi-finite integrals (better numeric convergence)

→ MIs are calculated numerically with SecDec

- Total CS: Corrections from LO to NLO are large (Kf=1.8)
  NLOfull w.r.t. NLOheft = +9%
- $p_{t,H}$ The bands of scales variation at NLO do not overlap anymore for $p_{t,H} \geq 340$ GeV
  But agreement if EFT rescaled with the full LO
- TOP mass renormalised in OS scheme

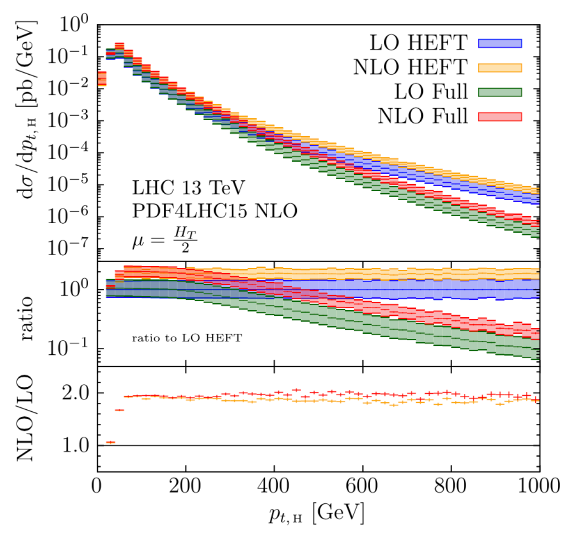

H+jet

- H+j was computed at NLO in QCD with the full dependence on TOP and BOTTOM masses

  R.B., V. Del Duca, H. Frellesvig, M. Hidding, V. Hirschi, F. Moriello, G. Salvatori, G. Somogyi, F. Tramontano, PLB 843 (2023) 137995

  - Master Integrals computed using differential equations solved in expansion
  - Renormalization of the Amplitude done in two different schemes:
    - External fields are renormalised on-shell. α_S is renormalised in a mixed scheme in which light-flavor contribution in $\overline{\mathrm{MS}}$ and heavy-flavor contrib at zero momentum
    - TOP-quark mass and Yukawa OS. TOP-quark mass and Yukawa in $\overline{\mathrm{MS}}$
    - TOP and BOTTOM masses and Yukawas in $\overline{\mathrm{MS}}$
  - Two-Loop 2 -> 2 and One-Loop 2 -> 3 are IR div. We combine them using Dipole Subtraction
  - Several checks at the level of the masters (with AMFlow) and the amplitude
    - Behaviour of the Two-Loop 2 -> 2 amplitude in the soft and collinear limits of one unresolved parton against factorisation formulas
    - Very large pt against Kudashkin-Melnikov-Wever
    - CS and pt for TOP against Chen-Huss-Jones-Kerner-Lang-Lindert-Zhang
  - In the case of $\overline{\mathrm{MS}}$ masses: dynamical evaluation in each point of phase space
  - Implementation in MADGRAPH5_aMC@NLO

H+jet

$$G_F = 1.16639 \cdot 10^{-5}\,\text{GeV}^{-2} \quad m_H = 125.25\,\text{GeV} \quad m_t^{OS} = 172.5\,\text{GeV}$$
$$m_t^{\overline{\text{MS}}}(m_t^{\overline{\text{MS}}}) = 163.4\,\text{GeV} \quad m_b^{\overline{\text{MS}}}(m_b^{\overline{\text{MS}}}) = 4.18\,\text{GeV}$$
$$\mu_R^0 = \mu_F^0 = \frac{H_T}{2} = \frac{1}{2}\left(\sqrt{m_H^2 + p_{t,H}^2} + \sum_i |p_{t,i}|\right)$$

NNPDF40_nlo_as_01180

Scale variation not shown

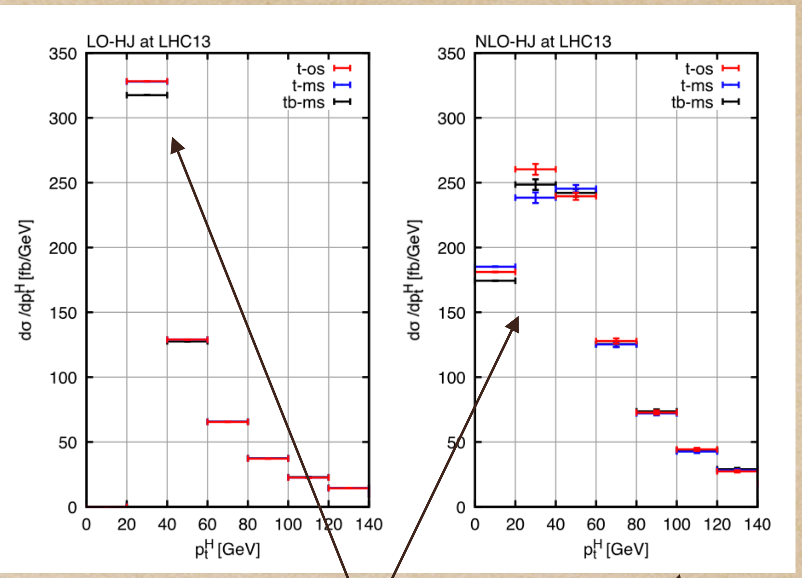

CS with pt>20 GeV

renormalisation of internal masses	σ_{LO} [pb]	σ_{NLO} [pb]
top+bottom–($\overline{\text{MS}}$)	$12.318^{+4.711}_{-3.117}$	$19.89(8)^{+2.84}_{-3.19}$
top–($\overline{\text{MS}}$)	$12.538^{+4.822}_{-3.183}$	$19.90(8)^{+2.66}_{-2.85}$
top–(OS)	$12.551^{+4.933}_{-3.244}$	$20.22(8)^{+3.06}_{-3.09}$

- The t-b interf changes the shape at low pt
- t-b interf irrelevant at medium-high pt (only TOP ok)

- Big K-factor (~ 2 at the diff level bin-by-bin)
- Scale uncertainty from 30% to 14%
- t-b interf. covers the gap from LO

LO NLO

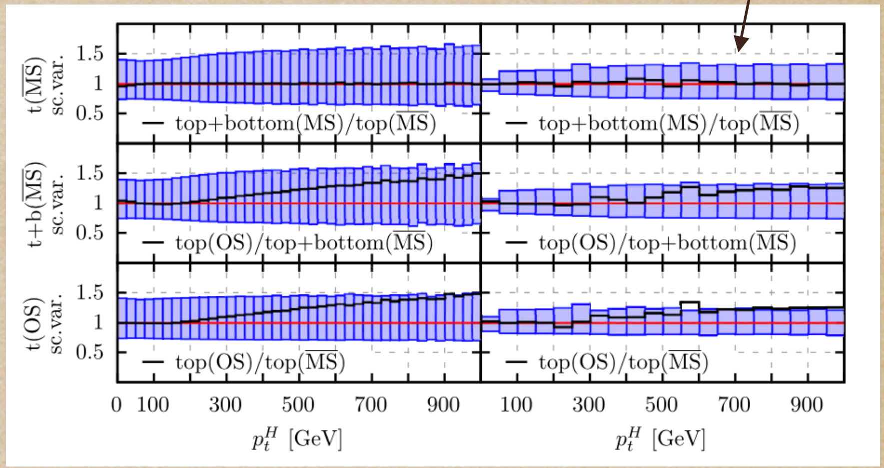

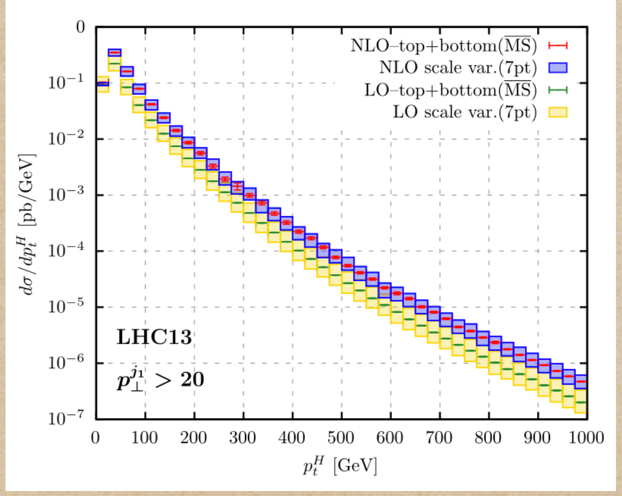

- Behavior of renormalization: $\overline{\text{MS}}$ falls off faster than OS
- Behavior less pronounced at NLO (as it should ...)

Some more details about the calculation:

QCD meets EW, CERN 5-9 February 2024

Theoretical framework: Perturbative QCD

At LHC hadronic collisions $h_1 + h_2 \to H + j + X$

we rely on Factorization Theorem

PDFs: Universal Part
Evolution with Fact scale predicted by the theory

Partonic CS: Process-dep Part
Calculation in PT Theory

$$\sigma_{h_1,h_2} = \sum_{i,j} \int_0^1 dx_1 \int_0^1 dx_2 \, f_{i,h_1}(x_1,\mu_F) \, f_{j,h_2}(x_2,\mu_F) \, \hat{\sigma}_{ij}(\hat{s}, m^2, \alpha_S(\mu_R), \mu_F, \mu_R)$$

NNLO
- S. Moch, J. Vermaseren, A. Vogt, Nucl. Phys. B688 (2004) 101
- A. Vogt, S. Moch, J. Vermaseren, Nucl. Phys. B691 (2004) 129

NNNLO
- S. Moch, B. Ruijl, T. Ueda, J. Vermaseren, A. Vogt, Phys. Lett. B782 (2018) 627
- J. Davis, B. Ruijl, T. Ueda, J. Vermaseren, A. Vogt, Nucl. Phys. B915 (2017) 335
- S. Moch, B. Ruijl, T. Ueda, J. Vermaseren, A. Vogt, JHEP 10 (2017) 041

Approximate NNNLO pdfs J. McGowan, et al. Eur. Phys. J. C. 83(3) (2023) 185

Exact Calculation: Partonic Cross Section

- Two-Loop 2 -> 2 interfered with the One-loop 2 -> 2

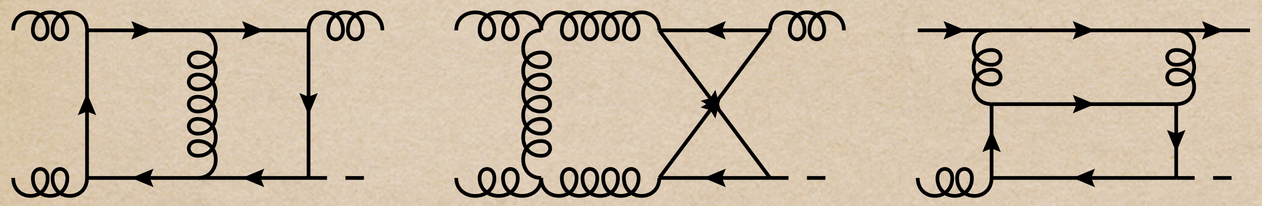

$$gg \to Hg$$
$$q\bar{q} \to Hg$$
$$qg \to Hq$$

- One-Loop 2 -> 3 interfered with the One-loop 2 -> 3

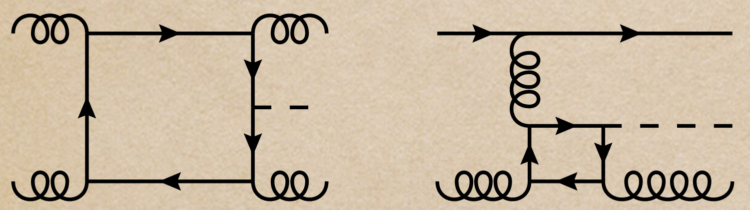

Computed with MCFM 9.1

V. Del Duca, W. Kilgore, C. Oleari, C. Schmidt, D. Zeppenfeld, PRL 87 (2001) 122001
L. Budge, J.M. Campbell, G. De Laurentis, R.K. Ellis, S. Seth, JHEP 05 (2020) 079
R.K. Ellis, S. Seth, JHEP 11 (2018) 006
J.M. Campbell, T. Neumann, JHEP 12 (2019) 034

- We renormalize UV divergences both in OS and/or in $\overline{\mathrm{MS}}$
- The two UV-ren sets are still separately IR divergent: we need IR counterterms in a subtraction scheme: we used Dipole Subtraction as implemented in MCFM 9.1

S. Catani and M. H. Seymour, Nucl. Phys. B 485 (1997) 291

Structure of the Amplitude

- Let us focus on the Two-Loop 2 -> 2 amplitude
- Kinematics: $H(p_4) \to g(p_1) + g(p_2) + g(p_3)$ $H(p_4) \to q(p_1) + \bar{q}(p_2) + g(p_3)$

$$s = (p_1 + p_2)^2 \, t = (p_1 + p_3)^2 \, u = (p_2 + p_3)^2 \, ; \quad p_1^2 = p_2^2 = p_3^2 = 0 \, ; \quad s + t + u = p_4^2$$

Integrals function of 3 dimless var: $x_1 = \frac{s}{m_t^2} \, ; \; x_2 = \frac{t}{m_t^2} \, ; \; x_3 = \frac{p_4^2}{m_t^2}$

- The H -> 3g amplitude can be expressed in terms of 4 form factors while the H -> gqqbar amplitude in terms of 2 form factors

T. Gehrmann, M. Jaquier, E. W. N. Glover, A. Koukoutsakis, JHEP 02 (2012) 056

H -> 3g $\mathcal{M}^{\mu\nu\rho} = A_{212} T_{212}^{\mu\nu\rho} + A_{332} T_{332}^{\mu\nu\rho} + A_{311} T_{311}^{\mu\nu\rho} + A_{312} T_{312}^{\mu\nu\rho}$

H -> gqqbar $\mathcal{M}^{\mu} = A_1 T_1^{\mu} + A_2 T_2^{\mu}$

- We project the contributions of the Feynman diagrams to the different FF

$$\mathcal{P}_i \cdot \mathcal{M} = A_i$$

where the A_i are expressed in terms of dim reg scalar integrals and then at every order in α_S we have $A_i = A_i(x_1, x_2, x_3, \epsilon)$

Structure of the Amplitude

- Color structure (Hggg)

$$A_i^{NLO}(x_1,x_2,x_3) \propto N_c\, A_{i1}^{NLO}(x_1,x_2,x_3) + A_{i2}^{NLO}(x_1,x_2,x_3) + \frac{1}{N_c}\, A_{i3}^{NLO}(x_1,x_2,x_3)$$

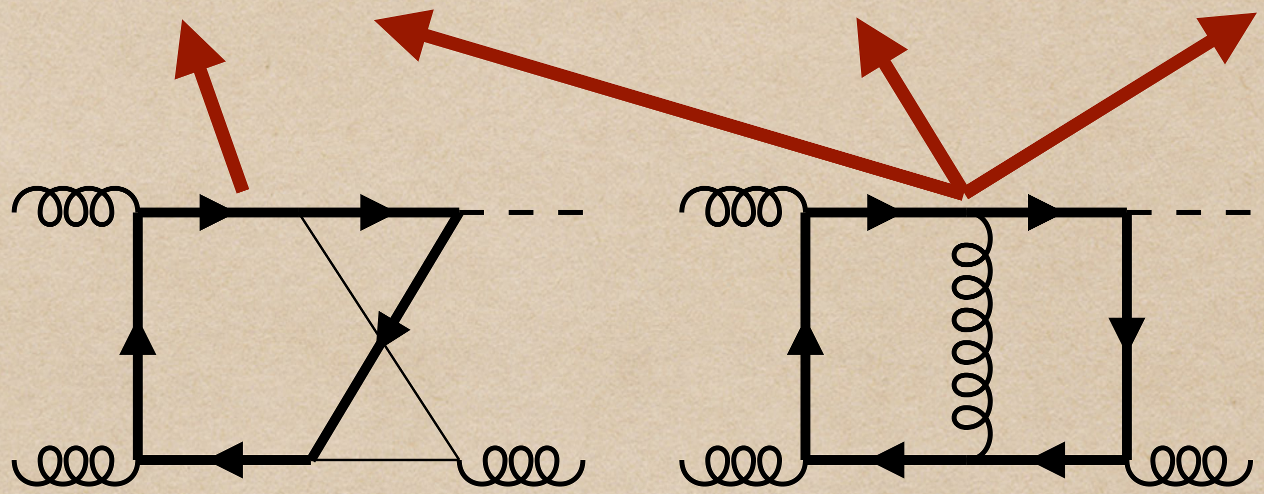

The planar diagrams contribute to the 3 FF while the crossed only to the leading color

Computation of the Amplitude

... goes through the “usual” steps:

- Generation of the Feynman diagrams: QGRAF and FeynArts

  P. Nogueira, J. Comput. Phys. 105 (1993) 279

  T. Hahn, Comput.Phys.Commun. 140 (2001) 418-431

- We computed the Form Factors projecting the single Feyn diags: FORM

  B. Ruijl, T. Ueda and J. A. M. Vermaseren, 1707.06453

- We can renormalize in different schemes. We always renormalize ext fields on-shell. α_S is renormalized in a mixed scheme with light-flavor contrib in $\overline{\text{MS}}$ and heavy-flavor at zero momentum. Masses are renormalized in OS or in $\overline{\text{MS}}$

- The Dim-Regularized scalar integrals were reduced to the MIs using IBP identities as implemented in KIRA and FIRE

  P. Maierhoefer, J. Usovitsch and P. Uwer, Comp. Phys. Commun. 230 (2018) 99

  J. Klappert, F, Lange, P. Maierhoefer and J. Usovitsch, Comput.Phys.Commun. 266 (2021) 108024

  A. A. V. Smirnov, JHEP 10 (2008) 107

  B. A. V. Smirnov, F. S. Chuharev, Comput. Phys. Commun. 247 (2020) 106877

Topologies and Master Integrals

- The MIs belong to SIX 7-denominator topologies

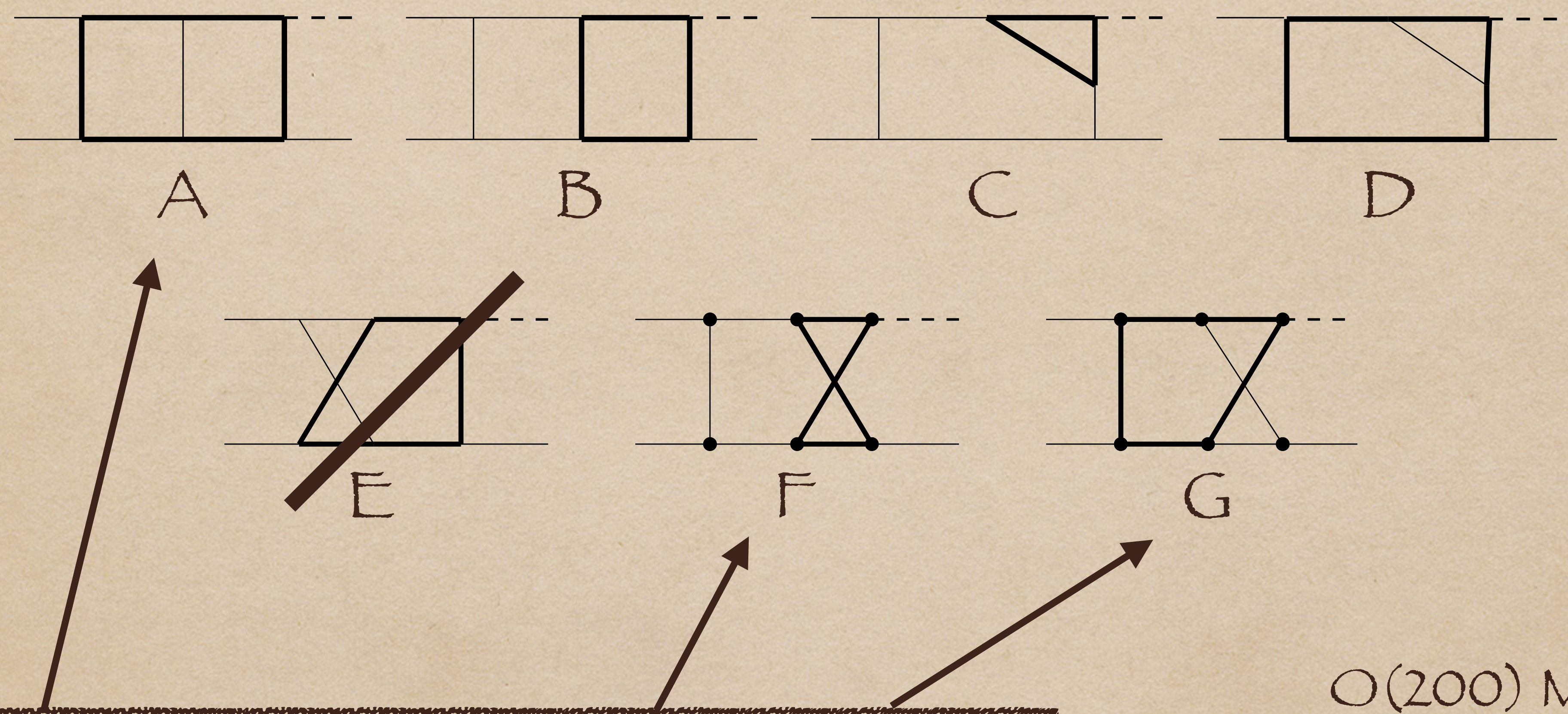

3 Topologies contain Elliptic sectors

O(200) MIs
O(20) elliptic
The rest Polylog

Master Integrals

- We divided the computation in three sets, corresponding to the various topologies

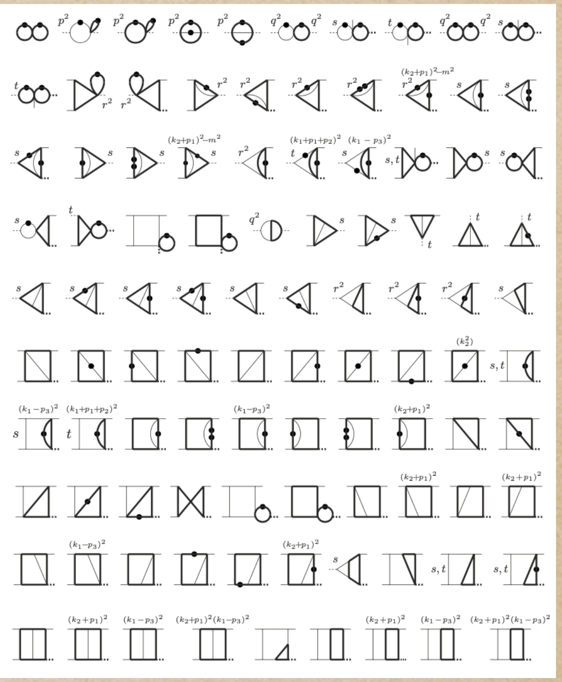

  - ✦ MIs for the planar topologies A, B, C, D. Analytic approach
    - All of them except 2 sectors with 4 MIs can be expressed in MPLs
    - MPLs sectors “effectively” written instead as a one-fold integration over weight-2 kernels
    - Elliptic sectors: repeated integrations of MPLs over ellipt. kernels

R.B.,V. Del Duca, H. Frellesvig, J. M. Henn, F. Moriello, V. A. Smirnov, JHEP 12 (2016) 096

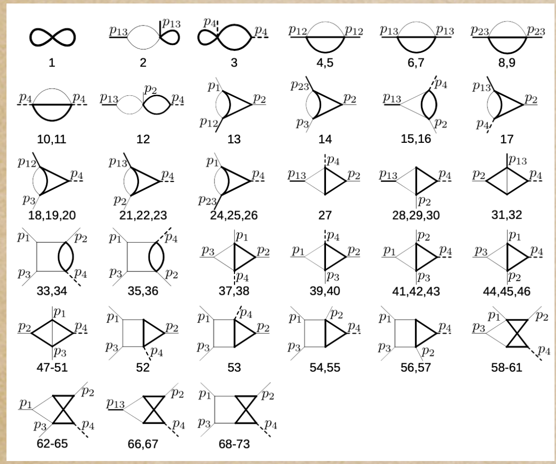

- ✦ MIs for the crossed topology G
  - Solved by series expansions

R.B.,V. Del Duca, H. Frellesvig, J. M. Henn, M. Hidding, L. Maestri, F. Moriello, G. Salvatori, V. A. Smirnov, JHEP 01 (2020) 132

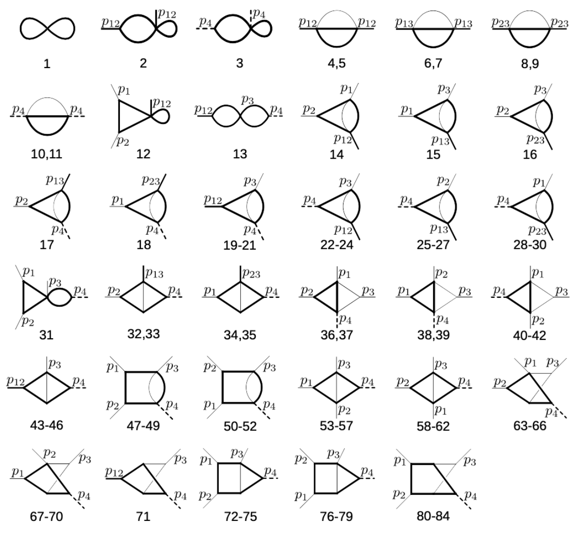

- ✦ MIs for the crossed topology F
  - Solved by series expansions

H. Frellesvig, M. Hidding, L. Maestri, F. Moriello, G. Salvatori, JHEP 06 (2020) 093

Elliptic sectors:
A - Homog. Eq. Elliptic; Non-Homog. polylogarithmic
B - Homog. Eq. Polylog: Non-Homog. Elliptic

Differential Equations

- The MIs were computed using the Differential Equations Method

$$\frac{\partial}{\partial x_i} f(x,\epsilon) = A_{x_i}(x,\epsilon)\, f(x,\epsilon)$$

V. Kotikov, Phys. Lett. B 254 (1991) 158
Z. Bern, L. J. Dixon and D. A. Kosower, Nucl. Phys. B 412 (1994) 751
E. Remiddi, Nuovo Cim. A 110 (1997) 1435
T. Gehrmann and E. Remiddi, Nucl. Phys. B 580 (2000) 485

- The system of differential equations was put (where possible) in canonical form

$$df(x,\epsilon) = \epsilon\, dA(x)\, f(x,\epsilon)$$

J. M. Henn, Phys. Rev. Lett. 110(2013) 251601
M. Argeri, S. Di Vita, P. Mastrolia, E. Mirabella, J, Schlenk, U. Schubert and L. Tancredi, JHEP 03 (2014) 082

- Although in "polylogarithmic form, square roots prevent a simple solution in iterated integrations. We found weight-2 in Polylog form and expressed weight-4 as a one-fold integration

C. Duhr, H. Gangl, J. R. Rhodes, JHEP 10 (2012) 075
S. Caron-Huot and J. M. Henn, JHEP 06 (2014) 114

- The elliptic sectors where evaluated solving Second-order linear diff eqs that revealed a good behaviour if combined in parametric form

Solution: $\int_0^1 \mathcal{F}(\alpha)\,\{K^i(\alpha), E^i(\alpha)\}\, d\alpha$

Difficult analytic continuation .... Series exp

Differential Equations: Semi-analytic evaluation

In some cases it is difficult to find closed-form solutions for the differential equations
What can be done is a solution of the relative differential equation in series expansion

S.Pozzorini and E. Remiddi, Comp. Phys. Comm. 175 (2006) 381

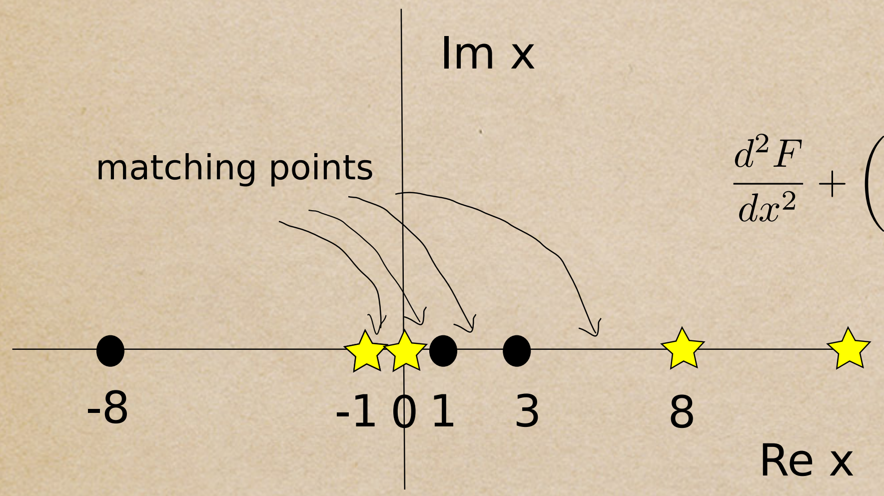

$$\frac{d^2F}{dx^2} + \left(\frac{3}{x} + \frac{1}{x+1} + \frac{1}{x-8}\right)\frac{dF}{dx} + \left[\frac{1}{x^2} + \frac{9}{8x} - \frac{4}{3(x+1)} + \frac{5}{24(x-8)}\right]F = \Omega(x)$$

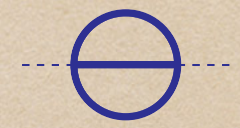

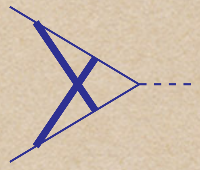

$$x = -\frac{s}{m^2}$$

- The differential equation and the solution are expanded in series around the singular points Every series depends on two arbitrary constants. Imposing the matching we express all of them in terms of the two constants
- Imposing initial conditions we fix the two constants. One can construct a numerical routine that evaluates F(x) for every value of x with arbitrary precision !!
- The convergence can be improved adding series expansions in intermediate regular points

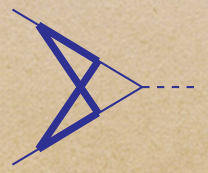

U. Aglietti, R.B., L. Grassi and E. Remiddi, Nucl. Phys. B 789 (2008) 45
R. N. Lee, A. V. Smirnov and V. A. Smirnov, JHEP 03 (2018) 008
R.B., G. Degrassi, P. P. Giardino and R. Groeber, Comp. Phys. Comm. 241 (2019) 122

Example: elliptic vertex for ttbar production

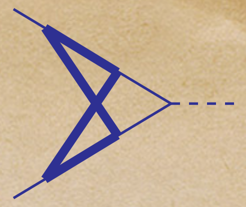

$$\begin{cases} \dfrac{dM_9}{dx} = -\dfrac{2}{x}M_9 + \dfrac{4m^2}{x}M_{10} \\ \dfrac{dM_{10}}{dx} = -\dfrac{1}{16m^2}\left(\dfrac{1}{x} - \dfrac{1}{x-16}\right)M_9 - \left(\dfrac{1}{x} + \dfrac{1}{x-16}\right)M_{10} + \Omega_s(x) \end{cases}$$

$$x = -\frac{s}{m^2}$$

$$\frac{d^2M_9}{dx^2} + \left(\frac{4}{x} + \frac{1}{x-16}\right)\frac{dM_9}{dx} + \left(\frac{9}{4x^2} - \frac{7}{64x} + \frac{7}{64(x-16)}\right)M_9 = \Omega(x)$$

Solution in $x = 0$

$$M_9^{(0)} = x^\alpha \sum_{n=0}^{\infty} a_n x^n \qquad \left(\alpha + \frac{3}{2}\right)^2 = 0$$

- Homogeneous solutions $M_9^{(0)}(x) = \frac{1}{\sqrt{x}} \sum_{n=-1}^{\infty} a_n x^n + \frac{\log x}{\sqrt{x}} \sum_{n=-1}^{\infty} b_n x^n \qquad a_0 = \frac{1}{64}a_{-1} + \frac{1}{32}b_{-1}\,, \quad b_0 = \frac{1}{64}b_{-1}$

  two independent solutions with $\begin{cases} a_{-1} = 1\,,\ b_{-1} = 0 \\ a_{-1} = 0\,,\ b_{-1} = 1 \end{cases}$

- Particular solutions $\Omega(x) = \sum_{n=-2}^{\infty} k_n x^n + \log x \sum_{n=-2}^{\infty} r_n x^n \qquad \tilde{M}_9(x) = \sum_{n=-1}^{\infty} p_n x^n + \log x \sum_{n=-1}^{\infty} q_n x^n$
- Matching with initial condition in $x = 0$ (only log) $M_9(x) = \sum_{n=0}^{\infty} p_n x^n + \log x \sum_{n=0}^{\infty} q_n x^n$
- The same in $x = 16$ + matching with the series in $x = 0$ … and so on
- Analitic continuation

L. Tancredi, A. Von Manteuffel, JHEP 06 (2017) 127

R.B., G. Degrassi, P. P. Giardino and R. Groeber, Comp. Phys. Comm. 241 (2019) 122

Differential Equations: Semi-analytic evaluation

- The examples above are one-dimensional, but the approach can be generalised to more dimesions and used for a general system of differential equations for the MIs
- The differential equations in s and t are combined and a one-dim diff eq is recovered and solved along a contour connecting two fixed points in the s-t plane

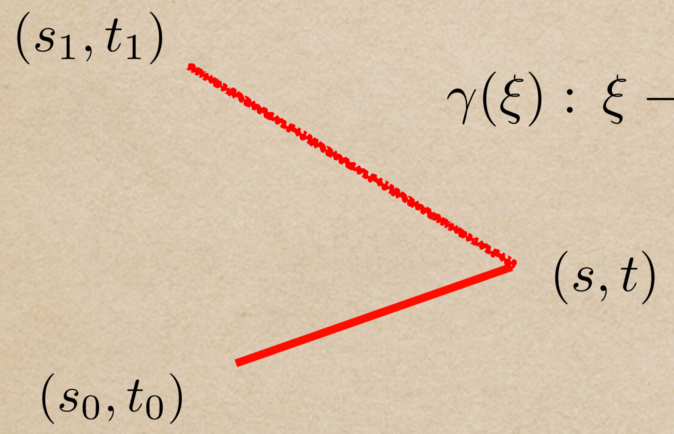

$$\gamma(\xi) : \xi \to \{s(\xi), t(\xi)\}$$

$$\frac{d}{d\xi} f(\xi, \epsilon) = A(\xi, \epsilon)\, f(\xi, \epsilon)$$

$$f(\xi, \epsilon) = \sum_{i=0}^{N} f^{(i)}(\xi)\epsilon^i$$

$$f^{(i)}(\xi) = \sum_{j=0}^{\infty} c^{(i,j)}(\xi - \xi_0)^j$$

$$f^{(i)}(\xi) = \sum_{j_1 \in S_1} \sum_{j_2=0}^{\infty} \sum_{j_3=0}^{\infty} c^{(i,j_1,j_2,j_3)}(\xi - \xi_0)^{w_{j_1}+j_2} \log^{j_3}(\xi - \xi_0)$$

- Analytical continuation is done expanding in the singular point and matching the series using Feynman prescription for the invariants
- The method is quite efficient and enables to compute fast a point in the phase space with arbitrary precision

F. Moriello, JHEP 01 (2020) 150

- Recently this method was implemented in a Mathematica code: DiffExp

M. Hidding, Comput.Phys.Commun. 269 (2021) 108125

Differential Equations: Semi-analytic evaluation

SeaSyde (Series Expansion Approach for Systems of Differential Equations)

- However DiffExp is designed for real masses. EW radiative corrections involve unstable particles Z, W, H, … : Complex Masses
- We developed an independent package, SeaSyde, to deal with series expansions solutions in the complex plane

$$z = -\frac{s}{m_V^2} \quad q = -\frac{t}{m_V^2} \qquad m_V^2 = M_V^2 - iM_V\Gamma_V$$

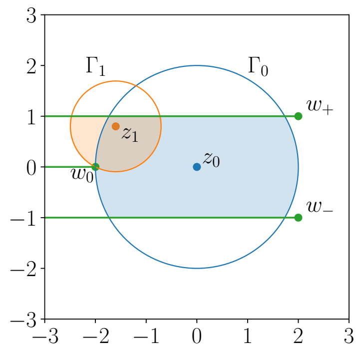

- Now we have cuts in the complex plane: we choose them to be parallel to the real axis, from the branching point to $-\infty$
- The path to avoid the cut proceeds via segments parallel to the real and to the imaginary axis in every complex variable, z and q
- We solve the equation in z, at fixed q (cuts in the complex z-plane) then the eq. in q at fixed z

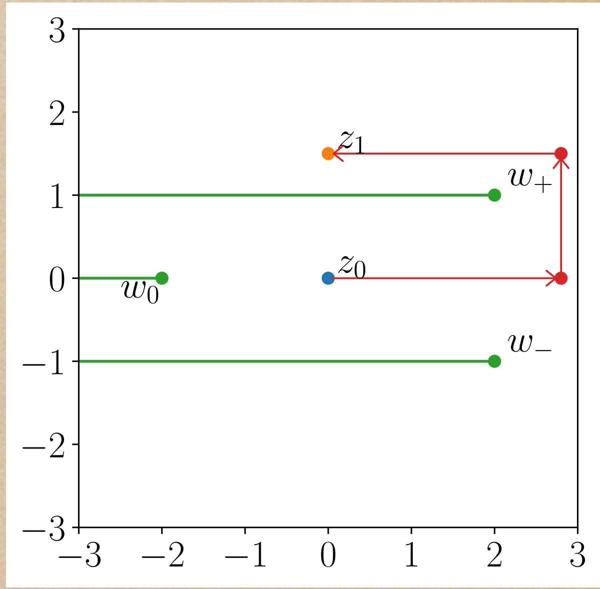

T. Armadillo, R.B., S. Devoto, N. Rana, A. Vicini, 2205.03345

Differential Equations: Semi-analytic evaluation

- The Strategy is to use semi-analytic evaluations to build a grid of points
- The simplest approach is "the snake", that can be used on a single core/single kernel computer: every point becomes the Initial condition for the following one

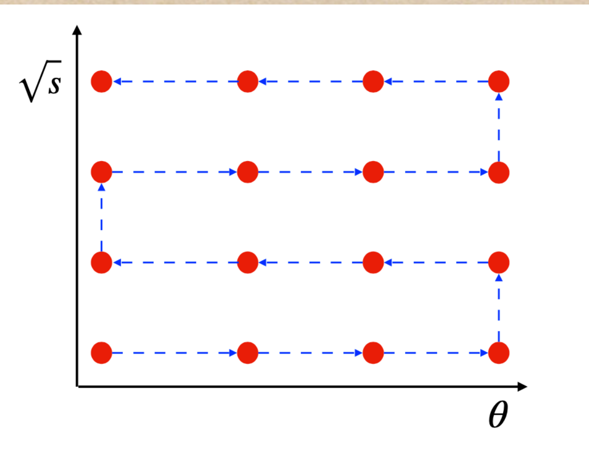

- Difficult parallelization: Mathematica kernels (and sub-kernels)
  Use of the sub-kernels: calculation of a line of points (high accuracy)
  And then each sub-kernel evolves a straight line in the other dimension

- Consider order of minutes for the evaluation of a single point:
  from 1 min to several, depending on the system and on the point …
  Need of many licences … break away from Mathematica ??

Problems to face …

- Size of the reduction/size of the coefficients: many MIs, complicated coefficients (many masses and invariants) of MB's
  - Possible simplifications: partial fractions "MultivariateApart", finite fields in "FiniteFlow"

M. Heller, A. Von Manteuffel, Comput. Phys. Commun. 271 (2022) 108174

T. Peraro, HEP 07 (2019) 031

  - Direct numerical evaluation of the reduction?
- Analytic Solution of the Differential Equations in presence of many invariants/masses
  - Although in the Polylogarithmic case … square roots -> difficult evaluation of a closed form
  - Although in closed form, problematic numerical evaluation: big formulas
  - Although in closed form, problematic numerical evaluation: big formulas
- Semi-Analytic Evaluation in principle no problem … in practice
  - Big systems -> large evaluation time
- Numeric evaluation (SecDec)?

Conclusions

- I do not have conclusions … at the moment we can apply what we learned so far to the EW challenge knowing that it will be even harder …

Thank you for your attention!